Fractured reservoir characterization using P-wave AVOA analysis of 3D OBC data

Stephen A. Hall, Heriot-Watt University, Edinburgh, U.K.
J-Michael Kendall, University of Leeds, Leeds, U.K.
Olav I. Barkved, BP Amoco Norge, Stavanger, Norway

Fracture systems can provide significant hydrocarbon storage and directional permeability so in many reservoirs their identification and characterization can be exploited to improve production and increase economic potential. For example, such information can be used to optimize production from horizontal wells by guiding their drilling perpendicular to aligned fracturing, which will generally provide higher yields than wells drilled parallel to fractures. Additionally fracture characterization could help guide waterflood-assisted production and identify compartments with good flow properties. Identification of such fracture systems is possible in 1D using core samples and well logs but, to fully optimize production of fractured reservoirs, it is desirable to understand the 3D distribution of fractures including the mapping of "swarms." These fractures are generally too small to be imaged using standard 3D seismic imaging techniques. However, they often occur in aligned sets and create anisotropy in seismic velocities (and permeabilities). Thus with true 3D seismic data such anisotropy and its spatial variability can be assessed, thereby providing insights into subseismic-scale fracturing.

The concept of fracture-induced anisotropy has been recognized for a long time although the potential for using the phenomenon to characterize fracturing in hydrocarbon reservoirs has only recently begun to be realized. This is largely through the development of new data acquisition techniques and production technologies (e.g., multicomponent true 3D seismic recording and horizontal drilling). On land, multicomponent and 3D acquisition have long been available but often limited by data quality and cost issues. Only a few examples of azimuthal anisotropy characterization using 3D surface seismic data exist. In the past decade such technologies have become commercially available for the marine environment through the development of ocean-bottom seismic (OBS) technology. True 3D marine seismic data acquisition has also become possible as a result of these OBS technologies and the first 3D OBS surveys were acquired in the mid-1990s. Prior to 3D OBS, multiazimuth marine seismic data and azimuthal anisotropy analysis were only possible with multiple 2D lines at different orientations.

This paper demonstrates, through a case study, the fracture-characterization potential of amplitude variation with offset and azimuth (AVOA) analysis with true 3D OBS data. Such an approach could ultimately allow mapping of directional permeability and stress throughout a reservoir via interpolation between direct measurements made at wells. Additionally some pitfalls associated with the interpretation of AVOA for fracture characteristics are highlighted. These issues are discussed with respect to a 3D ocean-bottom cable (OBC) data set acquired at Valhall Field in the Norwegian North Sea. The fundamentals of fracture-induced anisotropy and AVOA are first discussed before introducing the data example and AVOA processing. Finally the results from the AVOA analysis are interpreted with constraints from modeling to reduce ambiguity in AVOA interpretation, which has hitherto not been fully appreciated.

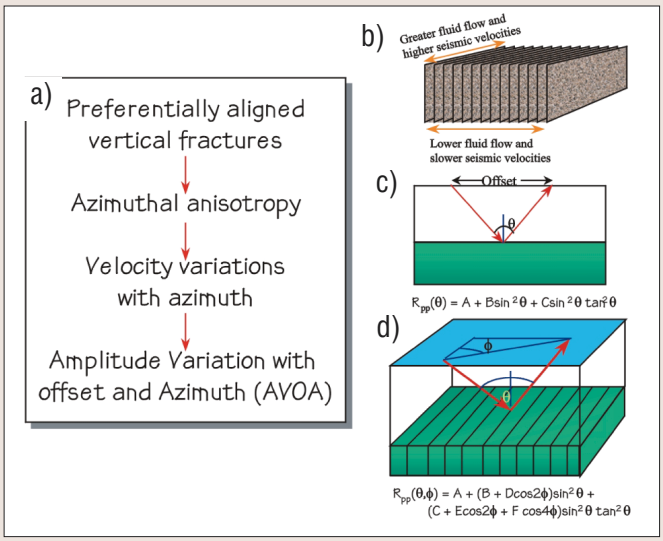

Figure 1. (a-b) The influence of aligned fractures on the elasticity and reflectivity of a medium. (c) Standard offset-dependent reflectivity and AVO equation. (d) Extension of the AVO concept and equation to AVOA.

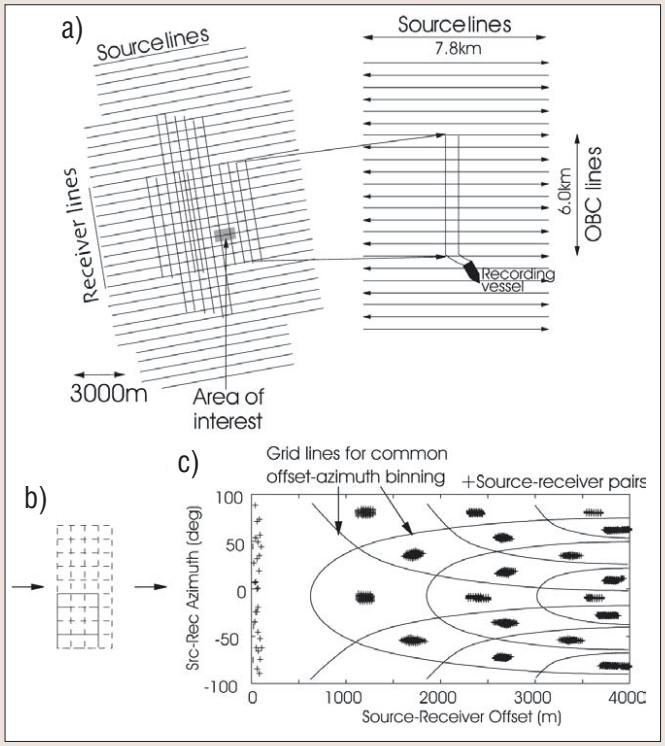

Figure 2. (a) Orthogonal source- and receiver-line acquisition of the Valhall 3D OBC data. (b) Schematic representation of the 3 × 3 macrobinning. (c) Patchy CMP offset-azimuth distribution that results from the sparse acquisition with the offset-azimuth bin-grid used to gather the data prior to AVOA analysis. The area of interest for the anisotropy analysis is highlighted in (a).

Anisotropy, fractures, stress, and AVOA. Anisotropy is defined as the directional variation of physical properties at a point within a medium. In the case of seismic anisotropy, this refers to variation in seismic velocity with direction (Figure 1), which can lead to measurable differences in traveltimes and reflectivity. In general, the observed anisotropy is an effective anisotropy, which exists when there is a preferential alignment of, for example, layers or fractures at a scale-length much smaller than the seismic wavelength. Preferential fracture alignment can also produce anisotropy in rock permeability so that seismic anisotropy and production may be linked (Figure 1b). Observation of a directional dependence in seismic properties could therefore provide the insight necessary to characterize fracture systems, stress anisotropy, and, potentially, preferential permeability directions.

Fractures are often subvertically aligned and thus produce *azimuthal anisotropy*—i.e., differences will be observed between seismic data acquired along different azimuths. The simplest case is the alignment of a single set of fractures where the anisotropy may be characterized by two principal directions, parallel and perpendicular to the direction of alignment. However fracture systems can be much more complex due to multiple alignments, such as conjugate shear sets, or different fracture-forming events and conditions. The alignment of open fracturing will also be influenced by the present-day stress field which can cause differential closure of fractures depending on their alignment relative to the main stress axes. The orientation of these stress axes may also show a regional trend or be perturbed locally around inhomogeneities such as faults and folds. All these factors will cause spatial variations in fracture character and alignment. Thus to fully characterize fracturing and stress, it is necessary to assess the anisotropy on a local scale and without prior assumptions about the likely orientation (e.g., based on regional information). Such a mapping of anisotropy may be achieved through observations of variations in seismic attributes such as traveltimes (including shear-wave splitting), velocities, or reflection amplitudes.

Amplitude variation with offset (AVO) analysis has for a long time been recognized as a useful indicator of lithology and pore fluid properties. Figure 1c shows the standard 2D AVO concept—the amplitude of a reflected wave varies as a function of incidence angle—through which significant insight into the character of the subsurface can be obtained from surface seismic data and the interpretation of AVO attributes such as the intercept and gradient terms.

In the presence of azimuthal anisotropy, the velocity of the media bounding an interface will have an azimuthal dependence and, therefore, the amplitude of waves reflected from such an interface will vary with the angle of incidence and also with azimuth (Figure 1d). Thus azimuthal anisotropy may be characterized using amplitude variation with offset and azimuth (AVOA). An advantage of considering reflection amplitudes, over traveltime and velocity methods, is that it is not necessary to have significant lithologic thickness to detect azimuthal variations in data. Thus AVOA provides good vertical resolution and also characterizes azimuthal attributes local to the reflector of interest. Traveltime or velocity analysis will show an accumulated effect through overlying layers.

In the simple situation involving only a single set of aligned vertical fractures, variations in amplitude can be described by linearized equations similar to those used for standard AVO analysis (Figure 1d). The azimuthal variation is expressed by coefficients which describe the 180° and 90° periodicity in amplitude (the $\cos 2\phi$ and $\cos 4\phi$ terms, respectively). The relative dominance of these terms is largely dependent on the properties of the fractures which induce the anisotropy. However, the $\cos 4\phi$ term is normally dominant at longer offsets and the azimuthal variations at short offsets are often treated as a $\cos 2\phi$ trend. Thus at near-offsets there will be two principal directions corresponding to the directions of maximum and minimum AVO along which two AVO gradient terms can be defined. These two new gradient attributes, aligned perpendicular and parallel to the direction of fracture alignment, characterize the fractures plus rock matrix and primarily matrix (approximately the isotropic part), respectively.

Valhall Field and data acquisition. Valhall Field, an Upper Cretaceous chalk reservoir, was discovered in 1975 and has been in production since 1982. Two reservoirs exist within the chalk group, Tor (0-60 m thick) and Hod (on average about 30 m thick). These reservoirs lie in a broad anticline overlain by the Tertiary shale of Lista formation, which together provide the trapping mechanism. The anticline is asymmetric and faulting (primarily extensional) has a dominant NNW-SSE orientation with some smaller faults WSW-ENE. The faults in the chalk do not in general extend far into the overburden and the Tertiary deposits show little structure.

Unfortunately the high potential of the reservoir in the form of significant oil-filled porosity (reaching 50% in some areas) is offset by poor matrix permeabilities. However, permeabilities up to an order of magnitude higher than those measured in core have been detected in production analysis (Ali and Alcock, 1994), suggesting that the potential recoverable yield could be increased. This enhanced permeability has been attributed to fractures, which are cited as the only possible means for efficient hydrocarbon production from the otherwise low-permeability chalk. Thus it is important to understand the distributions and characteristics of these small-scale fractures to optimize secondary production strategies such as waterflooding, but this will be difficult with standard seismic techniques. Mueller et al. (1997) observed anisotropy in dipole-sonic data that was attributed to alignment of fractures. Our aim is to characterize such anisotropy throughout the field using surface AVOA data in an effort to gain insight into the 3D fracture distributions.

Figure 2a outlines the acquisition of the 1997 Valhall 3D OBC data (Rosland et al., 1999). Patch shooting was used that involved 23, 7.8-km lines at 600-m spacing, with shots every 25 m, orthogonal to pairs of ocean-bottom receiver lines deployed 600 m separation. Receiver arrays were positioned at 25-m intervals along each 6-km receiver cable with seven 4C sensors at 1.5-m spacing in each group. Acquisition using such 3D OBS methods provides the potential for data rich in offset and azimuth content (i.e., "true 3D data" ideal for azimuthal analysis). However, although these data do have wide offset-azimuth coverage, such a 3D OBC acquisition provides a patchy data distribution (Figure 2c) which is not uniform in either offset or azimuth. Analyzing such data requires new data-analysis techniques.

AVOA analysis. Ideally AVOA analysis would consider common-azimuth (or common-offset) data for which separate AVO curves can be defined and compared. However, as highlighted above, these OBC data do not have uniform offset distributions in any azimuthal direction. One approach to address this would be to group or stack the data in common azimuth sectors, which would be the same for each sub-

surface position. Stacking in these bins would also provide improved signal-to-noise in often noisy data. However, to ensure a consistent and uniform offset sampling within these bins, 90° wide azimuth sectors, aligned either with the survey grid or to some assumed "regional" stress direction, are often used. Such binning will have the same periodicity as the AVOA effect of interest (Figure 3) and may lead to averaging out of the targeted azimuthal variations if the assumed orientation is incorrect or varies spatially. Smaller azimuth sectors will contain different offset distributions and an apparent anisotropy may be observed due to the varying offset sampling. Hall et al. (2000) presented an approach for prestack CMP-based AVOA analysis of OBC data (outlined in Figures 2 and 3) that avoids prior assumptions on orientation or azimuth binning that could bias the analysis. The main assumption in this approach is a cos 2ϕ azimuthal variation with azimuth but the AVOA is only analyzed in the near-offset range where this assumption is most valid, as discussed earlier, and such trends are also observed in the data.

The processing flow follows relatively standard but minimal preprocessing procedures to allow the prestack amplitudes and traveltimes to be picked in CMP gathers. Increased signal-to-noise may be achieved, without a loss of offset-azimuth character, by stacking the data into natural offset-azimuth groups (Figure 2c). Using overlapping 75 × 75 m CMP gathers with this common offset-azimuth grouping further improves the signal-to-noise. From these binned data a 2D Shuey-type AVO curve may be derived for each CMP to define the normal incidence amplitude and near-offset range (Figure 3a). For this defined near-offset range, the AVO gradient varies with azimuth by cos 2ϕ in the presence of azimuthal anisotropy (as shown in Figure 3b). Thus a best-fit surface, of the form given in Figure 1d, may be determined for each CMP from the AVO-derived normal-incidence amplitude and the near-offset amplitude data. Taking the initial AVO-derived normal-incidence term as prior information is more robust than deriving this in the surface fitting. Analysis of all CMPs in this way provides good spatial resolution of the reflector anisotropy. Figure 3c shows the major axes of the near-offset AVO gradient trend for each CMP in a small test area with the magnitude of the anisotropy indicated by the color contours. This map shows spatial variations in the anisotropy orientation and magnitude. A similar approach may be applied for traveltimes, using normal- or residual-moveout velocity (NMOA or RMOA) rather than AVO gradient, but this is in general more noisy than the AVOA. For the example here, picked horizon data are used, but the approach could be easily extended to 3D volumes.

Modeling and interpretation of AVOA. Figure 4 shows the results from numerical modeling of AVOA for the top chalk reflection at Valhall. This modeling uses an effective medium approach (outlined in Hall and Kendall, 2000) to describe the effective elasticity of a fractured medium for a single set of aligned fractures with a range of different properties. For this model, with brine-filled fractures, the "most-positive" near-offset AVO gradient is in the fracture normal direction. In contrast, the case with gas-filled fractures shows the "most-positive" near-offset AVO gradient parallel to fracture strike. Also, the long offset azimuthal variation in AVO is greater for gas-filled fractures than for brine-filled, but at shorter offsets the opposite is true. Thus the direction of most positive AVO gradient can change from fracture-strike to fracture-normal direction, with a change from gas to brine. In Figure 4b it can be seen that, at longer offsets, reflection amplitudes vary azimuthally with 180° and 90° periodicities but at near-offsets there appears to be just a 180° (cos 2ϕ) periodicity, as seen in the data and suggested by the

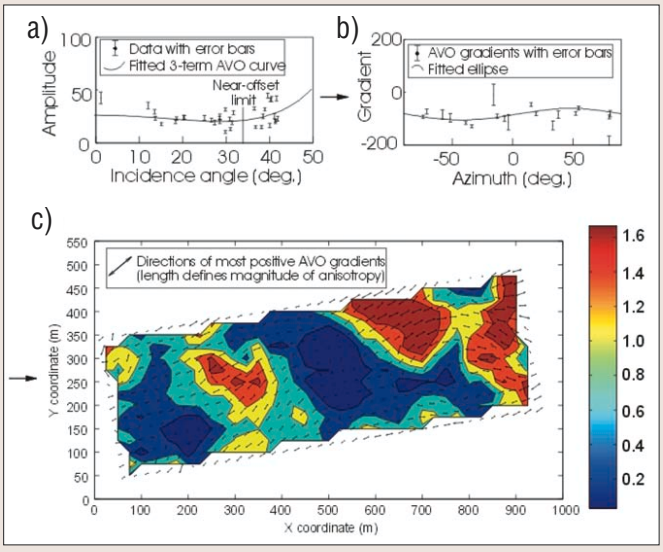

Figure 3. *(a) Diagram of AVOA analysis. (b) Shuey-type AVO curve fitting; scatter about the best-fit line looks like noise but derived AVO gradients for the near-offset data show a cos 2ϕ trend with azimuth. (c) Fitting an offset-azimuth surface to these data allows the AVOA to be assessed giving the principal directions and magnitude of anisotropy at each CMP (the magnitude is given as the normalized difference of the two principal gradients).*

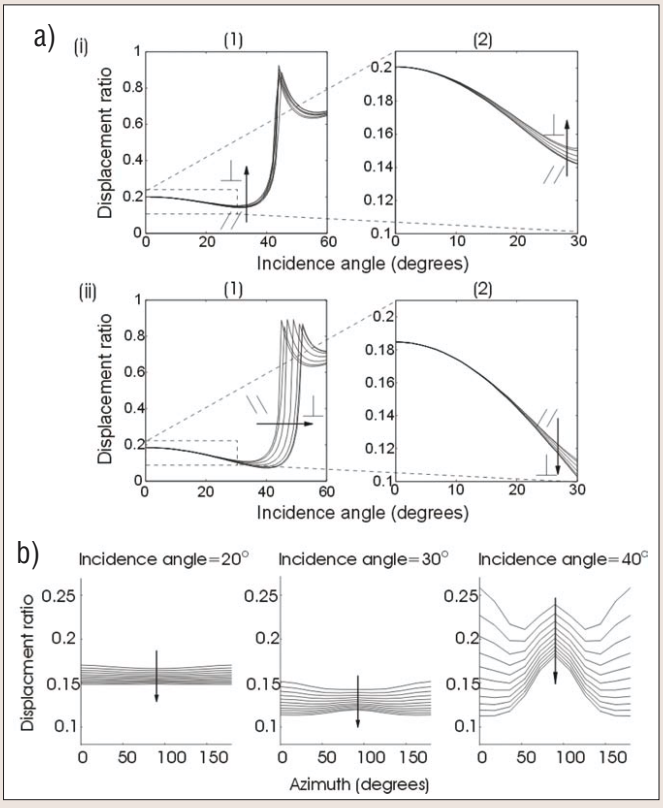

Figure 4. *(a) Modeled P-P AVO for the top-chalk reflection for 15° azimuth increments from the fracture strike direction to the fracture normal direction, as indicated by the arrows. i = brine-filled and ii = gas-filled fractures with a crack density of 0.1 and a fracture aspect ratio of 0.001. 1 = AVO for 0-60° angles of incidence which shows the P-P critical reflection as a large peak in the amplitude between 40° and 50°. 2 = Enlarged view of the AVO for 0-30° showing the change in AVO with azimuth over the near-offset range considered in the data analysis. (b) Modeled P-P AVAZ for different incidence angles and varying aspect ratios. Crack density is 0.1 with a brine-fill and aspect ratio increasing linearly from 0.0001 to 0.1 (indicated by arrows).*

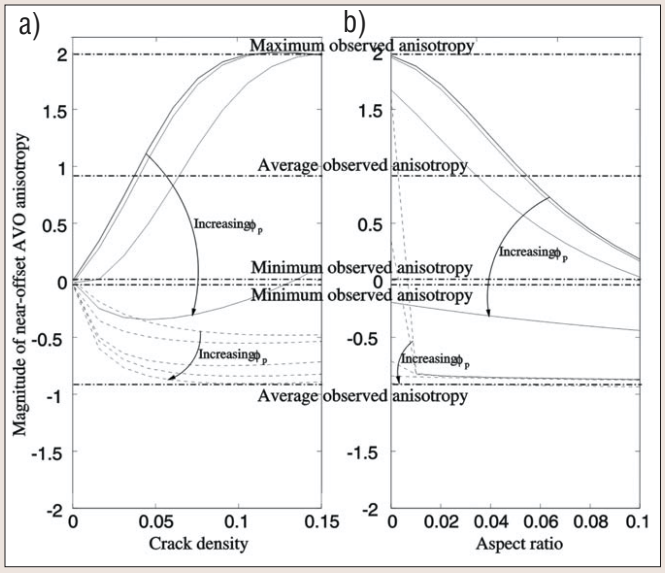

Figure 5. *Magnitude of modeled near-offset AVO-gradient anisotropy for different fracture models. Dashed lines are for gas-filled fractures and solid lines for brine-filled fractures. Anisotropy magnitude is plotted against (a) increasing crack density, with an aspect ratio of 0.001 and (b) increasing aspect ratio, with a crack density of 0.1, for different values of equant porosity; ϕp = 0.0, 0.0001, 0.001, 0.01, 0.1 with arrow indicating the direction of increase. The alignment of most-positive AVO gradient is in the fracture-normal direction for a positive anisotropy and the fracture strike direction for a negative anisotropy. The observed anisotropies in the data (the minimum and average values are indicated and the maximum observed anisotropy is about 2.0) may be positive or negative because the orientation of the fracturing is undefined. However, maximum anisotropy is only observed for models with a positive anisotropy. Thus, from modeling results, the anisotropy vectors in Figure 3c are inferred to be the fracture normal directions.*

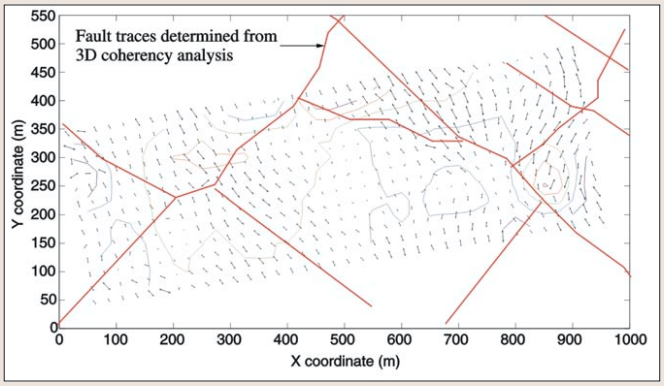

Figure 6. *Interpreted fracture map for the top chalk horizon compared to fault traces determined from coherency analysis with time contours at 18-ms intervals (red indicates deeper and blue shallower depths). This shows a good correlation of the inferred fracture patterns and the large-scale faulting with a greater alignment of the fractures near the NW-SE trending faults. In the SE corner, fracturing also appears perpendicular to the surface curvature defined by the time contours.*

equations in Figure 1. A key parameter that can influence the periodicity of the azimuthal variation and its polarity is the aspect ratio of the fractures, which is defined, for idealized ellipsoidal fractures, as the ratio of the short to long axes of the fracture. For low aspect ratio fractures the near offset trend is a positive cos 2ϕ variation with azimuth from the fracture normal whereas it may be negative cos 2ϕ for higher aspect ratios. For gas-filled fractures the change from a positive to negative azimuthal variation only occurs with very low aspect ratio (around 0.00025 compared to about 0.05 for brine-filled fractures). It is also interesting to note that, although the data being considered in the azimuthal

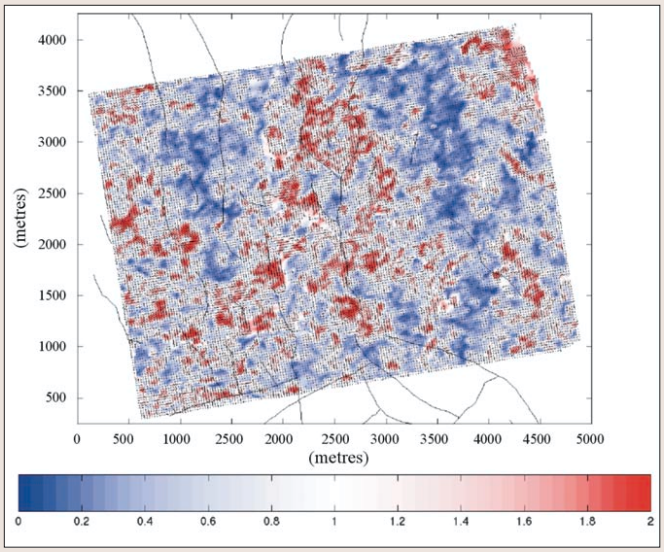

Figure 7. *Fracture orientations and anisotropy magnitude for the northern flank of the field derived from AVOA analysis (the magnitude is the normalized difference of the two principal gradients). Note the correspondence of both areas of high anisotropy magnitudes and the directions of fracturing with the large-scale faulting marked by the solid lines. The dominant direction of fracturing is NNW-SSE, roughly the main fault orientation.*

analysis only extend to about 30° incidence angle, the longer offset data (which are acquired but not used for the AVOA analysis) may contain significant information, which could further characterize the fracturing (i.e., the change from an approximately cos 2ϕ variation to a cos 4ϕ trend).

Thus there is a significant ambiguity in the interpretation of AVOA for fracture characteristics and it is possible that the fracture normal and fracture strike directions could be confused. Such confusion could, for example, lead to drilling a well parallel to fracturing and so not optimizing production. Such ambiguities in the interpretation of AVOA for fracture characteristics can be constrained by forward modeling. Figure 5 compares the AVOA magnitude data with synthetic AVOA magnitudes derived using an equivalent AVOA calculation to that used in the data analysis and for a range of effective fractured media. The high levels of observed anisotropy require the fractures to be liquid-filled with little communication of fluid with the matrix porosity. Furthermore it is seen that such models have positive azimuthal variations in AVO such that the AVO gradient will increase away from the fracture strike direction. Based on this modeling, fracture strike directions are inferred as orthogonal to the vectors in Figure 3c.

Fracture interpretation. Figure 6 shows the inferred fracture map from the AVOA data and modeling. Also plotted are the traces of faults (primarily normal) as determined from 3D coherency analysis. Correlation between AVOA-determined fracturing and large-scale faulting is observed with fractures aligned with the faults, as would be expected in the case of normal faults such as these. Additionally, greater alignment of fracturing appears along the NW-SE faults, suggesting a direction of maximum extension in this region is NE-SW (this is also apparent from magnitude of the anisotropy in Figure 3c).

Extension of this AVOA analysis to a larger area on the north flank of the field (Realey, 2000) showed similar trends with a dominant fracture orientation between 340° and 360° but with perturbations around larger faults (Figure 7). The observed dominant direction from this AVOA analysis is con-

sistent with independent data observations of Granger et al. (2000) and Caley et al. (2001). The former used amplitude ratios in mode-converted (P- to S-wave) reflections to estimate the orientation of the anisotropy. They used the same 3D OBC survey data in a similar area to that analyzed by Realey (2000) and found a dominant fracture direction between about 340° and 350°. Caley et al. (2001) considered shear-wave splitting in microseismic data acquired in the crestal region of the field just above the chalk. They found two fracture directions, one aligned with the AVOA results and another, more dominant trend, with an orientation at approximately 60° (i.e., about 90° from the main directions seen in the AVOA). This discrepancy possibly indicates that near the crest of the anticline, where the microseismic data were acquired, a different dominant stress regime exists to that on the flanks as might be expected in such a structure.

Summary. This paper has outlined the basics of AVOA analysis and demonstrated its potential, with application to true 3D OBC data, for fracture characterization. The main points are:

- True 3D OBS acquisition provides multioffset and multiazimuth data but, in the CMP domain, the offset-azimuth distribution is patchy and thus is not "full-offset and full-azimuth" data.
- Azimuth binning of such data improves the signal-to-noise but can destroy AVOA trends. However, signal-to-noise can be improved, without losing the offset-azimuth character, through binning of CMP data based on clusters in offset and azimuth. AVOA surface fitting of these offset-azimuth binned data can thus allow the azimuthal anisotropy to be properly assessed with few prior assumptions.
- On a local scale there can be significant variability in anisotropy orientation due, for example, to perturbation of stress fields around faults or across fold structures. Thus flexibility, such as avoiding prior assumptions about regional orientations, is necessary in the AVOA analysis.
- AVOA may be interpreted in terms of fracturing but ambiguity exists in this such that even the azimuth of fracturing could be misinterpreted. Thus forward modeling is necessary to resolve such ambiguity.
- At Valhall, AVOA analysis interpreted in terms of fracturing shows spatial variability in both orientation and magnitude that correlates with mapped faults and agrees with independent data observations. Further work is needed to fully interpret the fracturing from AVOA, which includes better constraints on the rock and fracture properties and improved understanding of the interrelationship of faults and fractures.

Although the approach and analysis shown here has been applied to an OBC data set it could be applied to any data set, land or marine, where there is true 3D acquisition, particularly when there is such a patchy offset-azimuth distribution. Furthermore these techniques may also be ideal for time-lapse seismic monitoring of changes in stress and fracturing through production because the anisotropic component of the rock mass is likely to be the most stress-sensitive and also control much of the permeability.

Suggested reading. Examples of land azimuthal anisotropy studies are Lynn and Thomsen (GEOPHYSICS, 1990); Lynn et al. (*TLE*, 1996); Mallick et al. (GEOPHYSICS, 1998; Gaiser et al. (SEG 2001 *Expanded Abstracts*); Gray et al. (*TLE*, 2002). Examples involving marine data are Harwood et al. (*Rev. Inst. Franc. Petr.*, 1998) and MacBeth et al. (*First Break*, 1999). AVOA theory and modeling are described by Ruger (GEOPHYSICS, 1998); Vavrycuk and Psencik (GEOPHYSICS, 1998); Hall and Kendall (9IWSA, 2000). Background on Valhall Field and 3D OBC data can be found in Ali and Alcock (*North Sea Oil and Gas Reservoirs II*, 1994) and Rosland et al. (EAGE 1999 *Extended Abstracts*). Detail on AVOA processing is given by Hall et al. (SEG 2000 *Expanded Abstracts*) and Hall and Kendall (under review for GEOPHYSICS). Complementary Valhall case studies have been published by Mueller et al. (EAGE 1997 *Extended Abstracts*); Realey (master's thesis, University of Leeds, 2000); Granger et al. (9IWSA, 2000); and Caley et al. (EAGE 2001 *Extended Abstracts*). TLE

Acknowledgments: The authors thank BP Amoco Norge AS and the Valhall partners (Amerada-Hess Norge AS, TotalFinaElf Exploration Norge AS, and Enterprise Oil Norge) for their support of this work and permission to publish the results. We also thank Leon Thomsen and Mike Mueller (BP) and Colin MacBeth (Heriot-Watt University) for their advice and support.

Corresponding author: steve.hall@pet.hw.ac.uk